Available online at www.sciencedirect.com
ScienceDirect
Journal of Photochemistry and Photobiology A: Chemistry 187 (2007) 275–284
Journal of Photochemistry and Photobiology A:Chemistry
www.elsevier.com/locate/jphotochem

Interactions of organic molecules at grain boundaries in ice: A solvatochromic analysis

Dominik Heger, Petr Klán *

Department of Organic Chemistry, Faculty of Science, Masaryk University, Kotlarska 2, CZ – 611 37 Brno, Czech Republic

Received 18 September 2006; received in revised form 12 October 2006; accepted 15 October 2006
Available online 10 November 2006

Abstract

Empirical solvent polarity parameters were used to evaluate the nature and magnitude of the intermolecular interactions of eight dipolar organic solvatochromic indicators in aqueous solutions frozen at 253 or 77 K, using the concept that is generally employed to study the polarity of liquid solvents or solid surfaces. $E_T(30)$, $E_T(33)$, and E_T^N as well as α, acceptor number (AN) (hydrogen-bond donation ability), β (hydrogen-bond acceptor ability), and π^* (polarity/polarizability) parameters were obtained by measuring the differences in the shifts of the absorption spectra of the probes. It was found that hydrogen-bond and electron-pair donating interactions were significant contributors to the polarity of a probe environment in ice and, at the same time, they were found to be substantially larger than those measured in liquid aqueous solutions and relatively insensitive to the sample temperature. While the former interaction type is attributed rather to the presence of water in a close vicinity of the probe molecules, the latter is evidently connected with the inter-probe interactions within the self-assembled molecular aggregations in conjunction with the water–probe interactions. The solvatochromic analysis revealed very weak dipole–dipole interactions (π^*) but the results are inconclusive. The data are consistent with a model according to which, upon freezing the aqueous solutions, the organic solute molecules are ejected to the grain boundaries to form highly concentrated liquid or frozen mixtures of organic and water molecules, having a high degree of complexity and exhibiting specific intermolecular interactions. Evaluation of the intermolecular polar interactions at the grain boundaries in ice should be of a great value in advancing our understanding of physical and chemical processes occurring in natural ice and snow.

Keywords: Ice; Solvatochromism; Polarity; Spectroscopy; Grain boundaries; Aggregation; Hydrogen bonding; Polarity; Polarization

1. Introduction

An understanding of the interfacial interactions between ice and organic molecules relies on a convergence of information from many different sources, including the studies of physical and chemical properties of the ice surface [1–9] or cryogenic chemical behavior of ice contaminants [10–18]. The surface of crystalline ice is a complex disordered system with a greater molecular mobility than that of bulk ice, the magnitude of which increases when contaminant molecules are incorporated [1]. It was shown that adsorption of various organic molecules on ice surface can be described well with a multiparameter linear free energy relationship, based on the van der Waals and the electron donor/acceptor interactions (such as H-bonding) [19]. The surface of ice and its interaction with contaminants has also been studied by infrared and Raman spectroscopy, combined with computer modeling, finding three different important types of surface water molecules, including those with dangling hydrogen or oxygen atoms [20,21]. The adsorbed states of some organic molecules, such as acetonitrile, chloroform [22], acetone [23], or benzene derivatives [24], were investigated by various techniques, such as desorption mass spectroscopy or electron spectroscopy, revealing the scope of hydrogen bonding or dipolar interactions. Most importantly, adsorption, desorption, interaction types, or diffusion of the molecules in ice are known to be temperature and phase-dependent variables [25–27]. Hydrophobic or hydrophilic solute molecules are known to become spontaneously segregated at grain boundaries in the polycrystalline ice during the freezing process [28,29]. Such a solute concentration-enhancing effect [26,30,31] may cause the solute organic molecules to self-organize [27]. There is still, however, a lack of information available to evaluate qualitatively the interactions of the organic molecules with water molecules at the grain boundaries in ice.

* Corresponding author. Tel.: +420 549494856; fax: +420 549492688.
E-mail address: klan@sci.muni.cz (P. Klán).

1010-6030/$ – see front matter © 2006 Elsevier B.V. All rights reserved.
doi:10.1016/j.jphotochem.2006.10.012

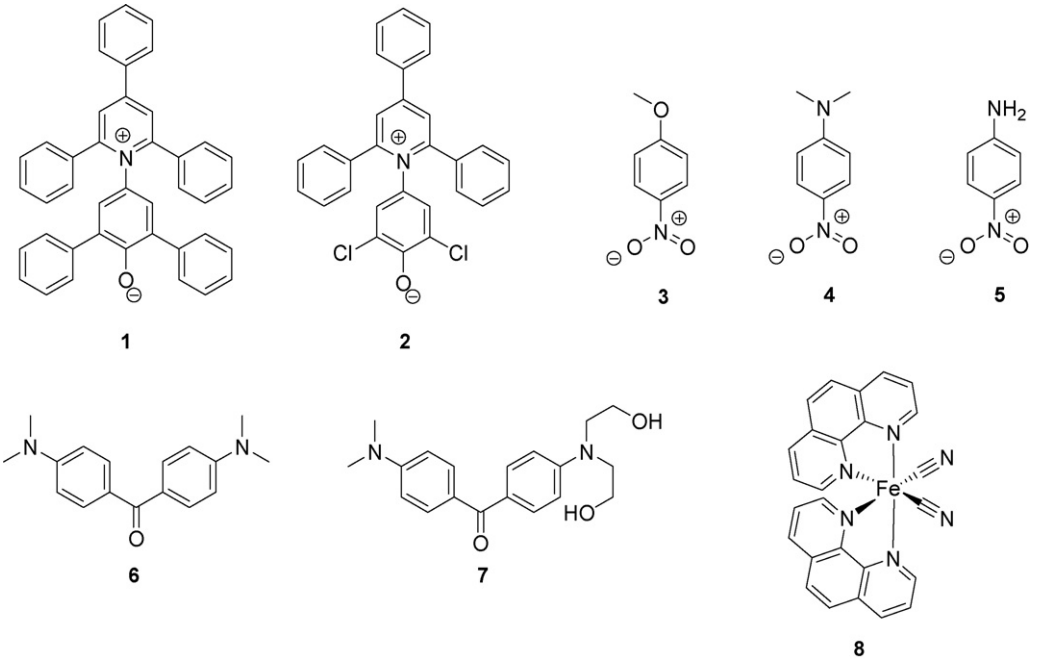

Chart 1. Solvatochromic probes.

Two limiting models for the behavior of a solidified *organic* solvent surrounding the solute as the temperature is lowered were proposed by Bublitz and Boxer [32]. In the first case, the distribution of polar solvent molecules around a solute could be approximately the same in both the liquid and solid states, because the probe–solvent interactions forces are already large in the solution. Any possible increase in solvent polarity was then suggested to be only due to the solvent contraction by freezing. In the second case, nonpolar solvent molecules in the vicinity of a solute could become locally more oriented by lowering the temperature to increase the intermolecular interactions. When these lower-energy configurations are frozen, a significant increase in (effective) polarity can be pronounced. Such an increase in polarity upon freezing has been experimentally observed for 2-methyltetrahydrofurane, toluene, and methylcyclohexane rather than for ethanol, which well supports the above mentioned assumption [32] or some other findings [33,34].

The above mentioned model is not, however, easily adopted for frozen *aqueous* solutions because (i) water is very polar; (ii) expands when it freezes [1]; (iii) hydrophobic organic solute molecules are not incorporated into the ice matrix [1,30,35]; but (iv) they are instead ejected to a (quasi)liquid/solidified layer [26] surrounding the ice crystals during the freezing process. We wished, therefore, to evaluate the nature and magnitude of the intermolecular interactions of dipolar organic chromophores in frozen aqueous solutions using the solvatochromic analysis, the concept that has already been extensively applied to study the polarity of liquid solvents [36–38], but also of the solid surfaces of silica [39–41], alumina [42], or α-amino acid crystals [43]. Empirical solvent polarity (solvatochromic) parameters are based on the spectroscopic measurements of changes in the absorption maxima of a probe. The solvatochromic effect originates from a different degree of orientation of solvent molecules around a dipolar ground state probe and the change in dipole moment when the chromophore is electronically excited [38]. Such a method, applicable for both liquid and solid phases, seemed to be an ideal tool to study the interactions at grain boundaries of ice.

Several different systems, exhibiting shifts of the UV–vis absorption maxima by changing the interaction forces between the solute and surrounding water molecules of ice, were employed in this work. $E_T(30)$, $E_T(33)$, and E_T^N values were obtained based on a correlation of the solvatochromic behavior of 2,6-diphenyl-4-(2,4,6-triphenyl-1-pyridinio)-phenolate (**1**) [38] and 2,6-dichloro-4-(2,4,6-triphenyl-1-pyridino)phenolate (**2**) [44] dyes, and the π^*, α, β, and acceptor number (AN) parameters were calculated based on a correlation of the solvatochromic behavior of 4-nitroanisole (**3**), *N*,*N*-dimethyl-4-nitroaniline (**4**), 4-nitroaniline (**5**) [45], 4,4′-bis(dimethylamino)benzophenone (Michler's ketone; MK) (**6**) [40], 4-(dimethylamino)-4′-[di(2-hydroxyethyl)-amino]benzophenone ($MK(OH)_2$) (**7**) [46], and *cis*-dicyano-bis(1,10-phenanthroline)iron(II) ($Fe(phen)_2(CN)_2$) (**8**) [40,47] dyes (Chart 1).

2. The study tools

Many different alternatives have been proposed to measure solute–liquid solvent interactions, resulting in a large variety of "solvent polarity scales", but still no general definition has emerged [48]. There are four reasonably independent parameters that can characterize the medium: hydrogen-bond donation ability (acidity) (α), hydrogen-bond acceptor ability (β), polarity/polarizability (π^*), and solvent stiffness (δ) [49].

The parameters were established by Kamlet and Taft in their simplified multi-parameter linear solvation energy (LSE) equation, $XYZ = XYZ_0 + s(\pi^* + d\delta) + a\alpha + b\beta$, where XYZ is a property of the solvatochromic probe (such as the wavelength of an absorption maximum) in the medium and XYZ_0 is that of a reference system [36]. The coefficients a, b, d, and s are solvent-independent correlation coefficients [50]. In this work, the α, β, and π^* parameters were used to study interactions of organic solutes at the grain boundaries in ice. In addition, the acceptor number parameter [49] has been obtained in order to determine the hydrogen-bond donation ability of the solvent independently on that of α.

2.1. Empirical solvent polarity parameters $E_T(30)$ and $E_T(33)$

The molar electronic transition energies $E_T(30)$ (Eq. (1)) of a dissolved probe **1** have been shown to correlate with α (hydrogen-bond donation ability) (~60%) and π^* (polarity/polarizability) (~40%) parameters (Eq. (2)) [38], while the β term (hydrogen-bond acceptor ability) was found to contribute scarcely to those values (vide infra) [38,49]. In addition to **1**, many other substitution derivatives were successfully employed as solvatochromic probes [38,51–53]. In this work, a dichloro derivative **2** ($E_T(33)$), was used because of its good aqueous solubility (3.7×10^{-4} mol L^{-1} at 25 °C [44]) and lower pK_a compared to $E_T(30)$ (p$K_a^{E_T(30)} = 8.64$; p$K_a^{E_T(33)} = 4.78$) [38]. The $E_T(33)$ scale is defined equally as that of $E_T(30)$ (Eq. (1)) and both scales can be interconverted according to Eq. (3) [44]. Besides, a normalized $E_T(30)$ parameter E_T^N was defined as a dimensionless quantity (Eq. (4)), and its values range between 0 for nonpolar TMS and 1 for highly polar water [38].

$$E_T(30 \text{ or } 33)\,[\text{kcal mol}^{-1}] = hc\nu_{max}N_A \quad (1)$$

$$E_T(30) = 31.2 + 15.2\alpha + 11.5\pi^* \quad (2)$$

$$E_T(30) = 0.979E_T(33) - 7.461 \quad (3)$$

$$E_T^N = \frac{E_T(30) - 30.7}{32.4} \quad (4)$$

2.2. The solvatochromic parameter π^*

This parameter measures the exoergic effects of dipole–dipole or dipole-induced dipole interactions among solute and solvent molecules, thus it evaluates the dipolarity and polarizability of the solvent [36]. A newly established and recommended probe is 4-nitroanisole (**3**) [45]. In case that its absorption band is not well resolved, the values of the absorption maxima of a secondary indicator, *N*,*N*-dimethyl-4-nitroaniline (**4**), are known to correlate with those of **3** by Eq. (5) [45]:

$$\tilde{\nu}(\mathbf{3}) = 0.6089\tilde{\nu}(\mathbf{4}) + 13840, \quad (5)$$

where $\tilde{\nu}$ is the wavenumber in cm^{-1}.

The π^* parameter is then calculated from $\tilde{\nu}$ of the absorption maxima according to Eq. (6):

$$\pi^*(\text{solvent}) = \frac{\tilde{\nu}(\text{solvent}) - \tilde{\nu}(\text{cyclohexane})}{\tilde{\nu}(\text{DMSO}) - \tilde{\nu}(\text{cyclohexane})} = \frac{\tilde{\nu}(\text{solvent}) - 34120}{31720 - 34120}, \quad (6)$$

where the corresponding $\tilde{\nu}$ were determined in cyclohexane, DMSO, and in a solvent to be studied, respectively [45].

2.3. The solvatochromic parameter α

This parameter is used to evaluate the solvent molecule as a hydrogen-bond donor. The calculation is based on the comparison of the solvent-induced absorption band maxima shifts of two similar probe molecules, from which one acts as a hydrogen-bond acceptor whereas the other cannot [38]. Here α is calculated by Eq. (7) using π^* and $E_T(30)$ [49]:

$$\alpha = 0.0649E_T(30) - 2.03 - 0.72\pi^*. \quad (7)$$

2.4. The solvatochromic parameter β

The ability of a solvent to act as a hydrogen-bond acceptor or electron-pair donor to the solute is frequently characterized by the β parameter [38]. Again, the solvatochromic comparison method is based on absorption behavior of two similar molecules, where one of them is capable of hydrogen bonding, whereas the other is not. For this work, *N*,*N*-dimethyl-4-nitroaniline (**4**) and 4-nitroaniline (**5**) pair of the probes [54,55] was applied and the β parameter was calculated according to Eq. (8):

$$\beta = \frac{\Delta\Delta\tilde{\nu}(\mathbf{4}, \mathbf{5})}{2759}, \quad (8)$$

where $\Delta\Delta\tilde{\nu}(\mathbf{4}, \mathbf{5}) = 0.9841\tilde{\nu}(\mathbf{4}) + 3490 - \tilde{\nu}(\mathbf{5})$, and $\tilde{\nu}$ is the wavenumber in cm^{-1} [54]. The β value is normalized to $\beta = 1$ in hexamethylphosphoramide [36,56].

2.5. The acceptor number AN

AN is an empirical parameter evaluating electron-pair accepting properties of the solvents that strongly correlates with the α parameter [49]. Its main advantage is that it can be determined from the spectrum of one compound only. The parameter is calculated from the absorption maxima of Fe(phen)$_2$(CN)$_2$ (**8**), in which the solvatochromic shift of the charge transfer band corresponds to a hydrogen-bond donation ability of this compound according to Eq. (9) [57,58]:

$$\text{AN}\,[\text{cm}^{-1}] = -133.8 + 0.00933\tilde{\nu}_{max}(\mathbf{8}). \quad (9)$$

AN can also be expressed as a function of α and $E_T(30)$ according to Eq. (10) [49]:

$$\text{AN} = -30.0 + 15.3\alpha + 1.01E_T(30). \quad (10)$$

2.6. The π^* and α parameters calculated using the probes **6**, **7**, and **8**

These parameters were calculated from the absorption maxima of MK (**6**), $MK(OH)_2$ (**7**) and $Fe(phen)_2(CN)_2$ (**8**) by Eqs. (11) and (12) according to Spange et al. [40]. Since the resolution of the absorption bands in the spectra of MK (**6**), which is not very soluble in water, was very poor in samples frozen at 253 K, $MK(OH)_2$ (**7**) was used instead as an alternative and the values of $\tilde{\nu}_{max}$(**6**) were obtained by a linear correlation of the values published for MK and $MK(OH)_2$ in 26 solvents [46] according to $\tilde{\nu}_{max}(\mathbf{6}) = -0.96 + 1.038\tilde{\nu}_{max}(\mathbf{7})$.

$$\alpha = -7.90 + (0.453\tilde{\nu}_{max}(\mathbf{8}) \times 10^{-3}) + (0.021\tilde{\nu}_{max}(\mathbf{6}) \times 10^{-3}), \quad (11)$$

$$\pi^* = 13.889 + (0.251\tilde{\nu}_{max}(\mathbf{8}) \times 10^{-3}) - (0.32\tilde{\nu}_{max}(\mathbf{6}) \times 10^{-3}). \quad (12)$$

3. Experimental

3.1. Chemicals

2,6-Diphenyl-4-(2,4,6-triphenyl-1-pyridinio)-phenolate (E_T (30); Aldrich; 90%), 2,6-dichloro-4-(2,4,6-triphenyl-1-pyridinio)phenolate (E_T(33); Fluka; >99%), 4,4′-bis(dimethylamino)benzophenone (Michler's ketone (MK); Aldrich, 98%), 4-(dimethylamino)-4′-[di(2-hydroxyethyl)-amino]benzophenone ($MK(OH)_2$) [59], 4-nitroanisole (Acros organics; >99%), 4-nitrophenol (Lachema; p.a.), 4-nitroaniline (Lachema, p.a.), *N*,*N*-dimethyl-4-nitroaniline (Acros organics; >99%), and *cis*-dicyano-bis(1,10-phenanthroline)iron(II) ($Fe(phen)_2(CN)_2$; Pfaltz and Bauer; >99%) were used without further purification. Each experiment was performed with a freshly prepared stock solution. Water was purified by the reverse osmosis process on an Aqua Osmotic 03 and its quality complied with U.S. Pharmacopaial Standards (USP).

3.2. Absorption measurements

The solidified samples containing probe solutions in Plastibrand cuvettes (transparent at >280 nm) were prepared by freezing either quickly at 77 K (a liquid nitrogen bath) or slowly at 253 K (an ethanol cooling bath). The absorption spectra of liquid aqueous solutions were measured on a Unicam UV4 spectrometer (Cambridge, UK) against a pure water sample in quartz cells with the optical path length of 1 cm. The absorption spectra of frozen samples and the reference spectra of pure ice were measured on a Lambda 19 UV–vis/NIR spectrophotometer (Perkin-Elmer) using a 60-mm integrating sphere (the slit width was set to 1 mm and the scan speed to 480 nm min^{-1} or lower) immediately after removing the cuvettes from the cold environment. Although the sample temperature was not controlled during the absorption measurements, no changes of the spectra were observed within the time period necessary for duplicate consecutive experiments. The averaged spectral background of pure ice was subtracted from each spectrum and the spectra shown are averaged from at least three independent measurements. The final spectra were smoothed using an adjacent averaging method when necessary. MATLAB and Origin were utilized as the graphical and statistical software. The step by step filter program [60,61] was applied to determine the number of peaks and λ_{max} in the spectra.

4. Results

The UV–vis absorption spectra of solvatochromic dyes in liquid and frozen aqueous solutions were measured and the corresponding absorption maxima (λ_{max}) are listed in Table 1. The samples were frozen either relatively slowly (253 K) or quickly (77 K), and the spectra of frozen samples, being warmed from 77 to 253 K or cooled down from 253 to 77 K, were also obtained. The latter experiments were performed in order to find if the spectral changes are reversible in this temperature range. These experimental conditions were selected based on our previous study of methylene blue aggregation [27], according to which a solute concentration enhancement at the grain boundaries of ice strongly depended on the sample temperature. Furthermore, the temperature of 77 K is unquestionably below the corresponding eutectic temperatures for all mixtures, while the probe molecules in highly concentrated layers covering the ice crystals at 253 K will exhibit considerable diffusion [27]. Changes in the magnitude of dye aggregation could undoubtedly affect nonbonding interactions among the probe and water molecules.

Figs. 1–5 show the spectra of the probes **2**, **4**, **5**, **7**, and **8**, which were used to determine the solvatochromic parameters. These dyes, listed in Table 1, were selected on the basis of

Table 1
The absorption maxima found in liquid (293 K) and frozen (253 or 77 K) aqueous solutions containing solvatochromic probes[a]

Probe	Concentration/mol L^{-1}	λ_{max} (nm) (293 K)	λ_{max} (nm) (253 K)	λ_{max} (nm) (77 → 253 K)[b]	λ_{max} (nm) (77 K)	λ_{max} (nm) (253 → 77 K)[c]
2	3.7×10^{-6}	406 (407 [44])	464, 512	467, 511	463, 509	466, 509
4	2.6×10^{-6}	421 (422 [62])	348	356	350	355
5	1.74×10^{-5}	378 (380 [36])	360	371	387	382
6	1.9×10^{-6}	379	n.d.	n.d.	369	362
7	2.62×10^{-5}	382 (383 [46])	373	379	371	369
8	1.13×10^{-6}	512 (510 [63])	463, 518, 583	465, 515, 573	469, 516, 572	467, 518, 570

[a] The values in the parenthesis are from the literature.
[b] The samples frozen at 77 K and warmed to 253 K.
[c] The samples frozen at 253 K and cooled to 77 K.

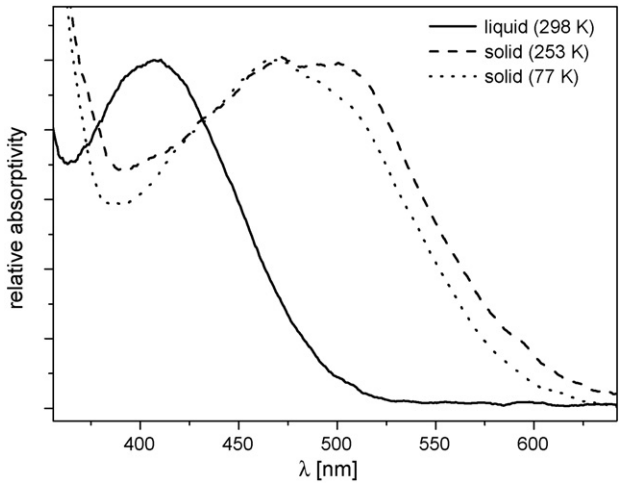

Fig. 1. The normalized absorption spectra of the aqueous solution of 2,6-dichloro-4-(2,4,6-triphenyl-1-pyridinio)phenolate (**2**) obtained at 298, 253, and 77 K.

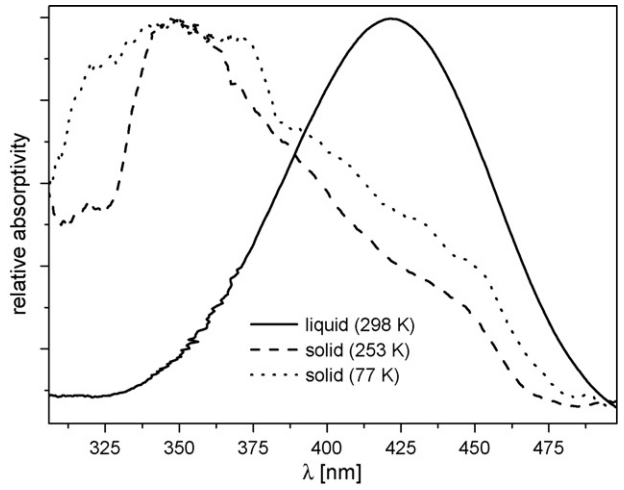

Fig. 2. The normalized absorption spectra of the aqueous solution of *N*,*N*-dimethyl-4-nitroaniline (**4**) obtained at 298, 253, and 77 K.

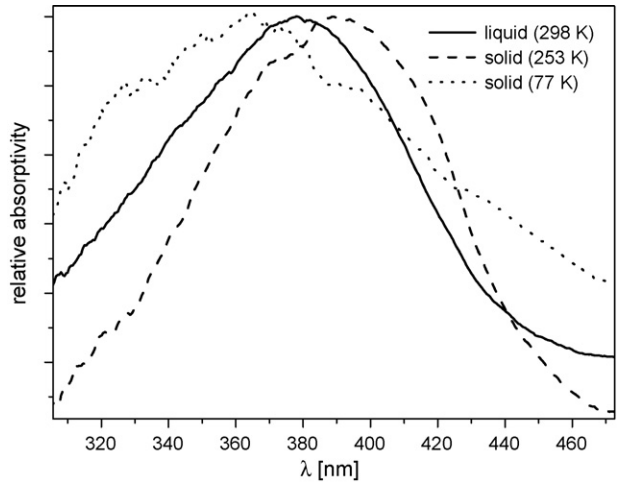

Fig. 3. The normalized absorption spectra of the aqueous solution of 4-nitroaniline (**5**) at 298, 253, and 77 K.

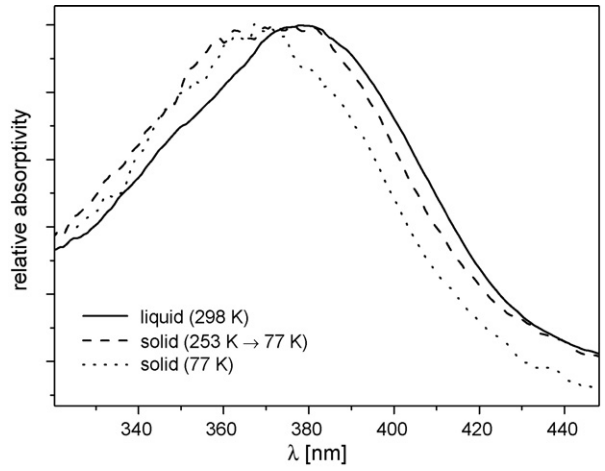

Fig. 4. The normalized absorption spectra of the aqueous solution of 4-(dimethylamino)-4′-[di(2-hydroxyethyl)-amino]benzophenone ($MK(OH)_2$) (**7**) obtained at 298, 253, and 77 K. (253 → 77 K): the samples were frozen at 253 K and cooled down to 77 K.

their properties, such as a higher solubility in water, and the solvatochromic parameters were calculated using the absorption maxima shifts directly or by the correlations with some other systems, commonly used for such a purpose. The concentrations of the probes were adjusted carefully to obtain signals, which are well resolved from the background of pure ice. Heterogeneity and lower transparency of the polycrystalline ice samples evidently decreased the signal-to-noise ratio and a band broadening was attributed partially to light scattering and reflection.

4.1. The $E_T(30)/E_T(33)$ parameter

2,6-Diphenyl-4-(2,4,6-triphenyl-1-pyridinio)-phenolate ($E_T(30)$; **1**) could not be used in our experiments because it is protonated ($pK_a^{E_T(30)} = 8.64$) at low aqueous concentrations ($\sim 10^{-6}$ mol L^{-1}) [38], causing the solvatochromic band to

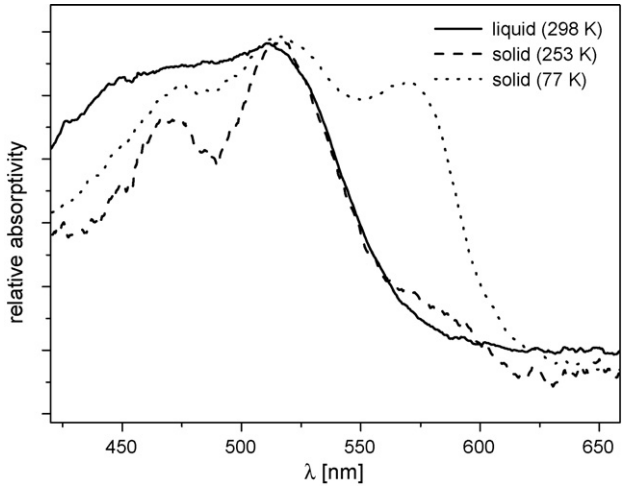

Fig. 5. The normalized absorption spectra of the aqueous solution of *cis*-dicyano-bis(1,10-phenanthroline)iron(II) ($Fe(phen)_2(CN)_2$) (**8**) obtained at 298, 253, and 77 K.

Table 2
The calculated solvatochromic parameters for liquid (298 K) and frozen (253 and 77 K) aqueous solutions[a]

Temperature (K)[b]	λ_{max}(**2**) (nm)[c] (abundances)	$E_T(33)$[d]	$E_T(30)$[e]	E_T^N[f]	π^*[g]	α[h]	β[i]	AN[j]
298	406	70.4 (70.2 [44])	61.5 (63.1 [38])	0.95 (1 [38])	1.15 (1.09 [64])	1.13 (1.17 [64])	0.15 (0.18 [64])	49.4 (54.8 [63])
253	464 (85%)	61.6	52.9	0.68	−0.12	1.48	1.45	46.1
	512 (15%)	55.8	47.2	0.51		1.12		34.8
77 → 253	467 (95%)	61.2	52.5	0.67	0.05	1.34	1.51	43.5
	511 (5%)	56.0	47.3	0.51		1.01		33.2
77	463 (95%)	61.8	53.0	0.69	−0.07	1.46	2.09	45.9
	509 (5%)	56.2	47.5	0.52		1.11		35.0
253 → 77	466 (89%)	61.4	52.6	0.68	0.03	1.36	1.82	44.0
	509 (11%)	56.2	47.5	0.52		1.03		33.8

Two values for the α parameter were obtained from two different λ_{max} values of $E_T(33)$.

[a] The parameter values for liquid solutions in the parentheses are from the literature.

[b] (77 → 253 K): the samples were frozen at 77 K and warmed to 253 K; (253 → 77 K): the samples were frozen at 253 K and cooled to 77 K.

[c] λ_{max} corresponding to the samples containing **2**. The values in the parentheses are the abundances of both resolved bands in the spectrum determined by the Gaussian curve fitting.

[d] The parameters were calculated according to Eq. (1) (probe **2**).

[e] The parameters were calculated according to Eq. (3) (probe **2**).

[f] The parameters were calculated according to Eq. (4) (probe **2**).

[g] The parameters were calculated according to Eq. (6) (probe **4**).

[h] The parameters were calculated according to Eq. (7) (probes **2** and **4**).

[i] The parameters were calculated according to Eq. (8) (probes **4** and **5**).

[j] The parameters were calculated according to Eq. (10) (probes **2** and **4**).

disappear. Instead, the $E_T(30)$ parameters were calculated using those of $E_T(33)$ according to Eq. (3). The changes in the absorption spectra of 2,6-dichloro-4-(2,4,6-triphenyl-1-pyridinio)phenolate ($E_T(33)$ probe; **2**) upon freezing (Fig. 1) were easily observed visually: a yellow liquid turned to a red ice sample. In contrast to the spectra obtained at 298 K, those measured at 253 or 77 K composed of two distinct absorption bands with λ_{max} equal to 464 and 512 nm, or 463 and 511 nm, respectively (Table 2). This may suggest that at least two species (e.g., different stable conformations of the probe; specific binding sites on the probe molecules) were observed after freezing the aqueous solutions. Conformational restriction, because of lower temperature and molecular confinement in the solid matrix, was highly probable especially in experiments at 77 K [18]. The calculation of the species abundance ratios, using the Gaussian fitting analysis [27], was based on the presumption that the species have similar absorption properties.

$E_T(33)$, and subsequently $E_T(30)$, were calculated using Eqs. (1) and (3), respectively, and they are shown in Table 2. In addition, the dimensionless E_T^N was derived according to Eq. (4). The bathochromic shifts [38] of both λ_{max} at low temperature imply that hydrogen-bond donation ability (α) and polarity/polarizability (π^*) of the frozen medium decreased compared to a liquid solution. Such lower values correspond to those of less polar solvents than water; for example, $E_T^N = 0.68$ and 0.52 was found for 1,3-butandiol [38] and 1-dodecanol [38], respectively. This simple comparison has, however, evidently no meaning when we wish to discuss the character of the interactions at the grain boundaries (vide infra). The temperature in the interval of 77–253 K had practically no effect on the E_T values; however, it did affect the abundances of the observed species to some extent.

4.2. The π^* parameter

We have attempted to determine the π^* parameter by measuring the absorption spectra of 4-nitroanisole (**3**) [45] but the corresponding solvatochromic band almost disappeared after the solution was frozen. Therefore, an alternative probe, *N*,*N*-dimethyl-4-nitroaniline (**4**) (Fig. 2), was used for π^* determination using a linear correlation (Eq. (5)) and consequently using Eq. (6). The absorption band λ_{max} of the frozen solutions was shifted hypsochromically by approximately 70 nm, comparing to liquid samples (Table 1), providing the π^* values close to 0 in all cases (Table 2). Extremely low values of π^* found in ice could be compared, for example, to those obtained in cyclohexane [64], which exhibits no dipole–dipole interactions toward this probe. It is apparent from the table that temperature had no effect on these values.

4.3. The α parameter

The α parameter was calculated from the preceding π^* and $E_T(30)$ values (Table 2) using Eq. (7). It was thus not surprising that the values, corresponding to the most abundant bands, were higher for ice samples in case that the corresponding π^* parameters were negligible. This parameter represents a principal interaction evaluated by $E_T(33)$, and was not also affected by temperature changes. For comparison, $\alpha = 1.4$ corresponds to that typically found in a strong hydrogen-bond donating solvent, such as trifluoroethanol ($\alpha = 1.51$) [64].

4.4. The β parameter

This parameter was calculated from the absorption maxima of *N*,*N*-dimethyl-4-nitroaniline (**4**) and 4-nitroaniline (**5**) (Figs. 2 and 3) according to Eq. (8) [56]. 4-Nitroaniline (**5**) is a homomorphic molecule to *N*,*N*-dimethyl-4-nitroaniline (**4**), being able to interact with hydrogen-bond acceptor solvents. The calculated values were found to be significantly higher in ice than those in liquid solutions. Being somewhat different in samples frozen quickly or slowly, the average β value of 1.7 is higher than that of any known solvent; a very high value ($\beta = 1.43$) was, for comparison, found in 1,2-diaminoethane [38]. Relative intensities of the solvatochromic band of **4** decreased in frozen solutions, producing some uncertainty in the interpretation of these data.

4.5. The alternative AN, α and π^* parameters

In addition, we wished to employ an independent procedure to evaluate AN, α and π^* parameters, using 4,4′-bis (dimethylamino)benzophenone (Michler's ketone) (**6**), 4-(dimethylamino)-4′-[di(2-hydroxyethyl)-amino]benzophenone dyes ($MK(OH)_2$) (**7**), and *cis*-dicyano-bis(1,10-phenanthroline)iron(II) ($Fe(phen)_2(CN)_2$) (**8**). This method was introduced by Spange et al. to evaluate polarity of various solid surfaces [40]. While the acceptor number can be determined directly according to Eq. (9), a linear correlation of λ_{max} (**7**) with those of **6** (vide infra) would enable us to calculate α and π^* using Eqs. (11) and (12) (not shown). $Fe(phen)_2(CN)_2$ in the liquid solution gave a broad asymmetric absorption band with $\lambda_{max} = 512$ nm (Fig. 5). Upon freezing the band was split in three distinct maxima at approximately 466, 517, and 580 nm (having the relative abundance ratio 4:5:1 at 253 K, determined by the Gaussian curve fitting). The λ_{max} values were almost independent on temperature; only a decrease in the intensity of the most shifted band (580 nm) was observed for the samples frozen at 253 K compared to those frozen at 77 K. In case that these three bands (Table 1) represent three species, the calculated AN values (Eq. (9)) would vary within a very wide interval (68, 46, 26, respectively). Since the spectrum of **8** in ice, however, resembles that of its crystalline form adsorbed on cellulose fiber surface [65], we can only speculate whether the parameter evaluation is physically justified.

The absorption bands of both MK (**6**) and $MK(OH)_2$ (**7**) shifted hypsochromically upon freezing comparing to water samples. The absorption spectra of **6** were not well resolved at 253 K, possibly because of its low aqueous solubility; therefore, the absorption maximum could not be determined. In contrast, the $MK(OH)_2$ spectra provided distinct absorption bands at both 77 and 253 K (Fig. 4) and no significant differences were found when the samples were frozen slowly or quickly.

4.6. Solvatochromic parameters in organic solutions

In order to estimate the parameter values for very concentrated probe solutions where the dipolar solvatochromic probes are expected to be largely segregated, the absorption maxima of **1**, **4**, and **5** in dichloromethane solution containing dye crystals (slurry) were compared to those obtained in dichloromethane diluted solutions (Table 3). The results show that all values changed when the concentration increased; a significant increase in the β value is the most apparent.

Table 3
The solvatochromic parameters obtained in CH_2Cl_2 diluted solutions and slurry[a]

Medium	$E_T(30)$	E_T^N	π^*	α	β
CH_2Cl_2[b]	40.7 [38]	0.31 [38]	0.82 [49]	0.13 [49]	0.10 [49]
CH_2Cl_2 slurry[c]	43.7	0.40	0.64	0.34	1.04

[a] Eqs. (1), (4), (6), (7) and (8) were used in the calculations.
[b] Diluted solutions; the data from the literature.
[c] A mixture of crystallized probe molecules in saturated solution.

5. Discussion

When an aqueous solution is frozen, the organic impurities are excluded from the bulk ice to the grain boundaries, causing a substantial increase in their local concentration [27]. The initial probe concentrations in water, $c = 10^{-5}$ to 10^{-6} mol L^{-1}, unquestionably increased locally upon freezing by many orders of magnitude [27] and the compounds could crystallize or form an aqueous organic glass microscopically interspersed in a polycrystalline ice matrix, as suggested by Guzman et al. in case of frozen pyruvic acid solutions [17]. As a result, two kinds of interactions have to be considered: interactions of the probe molecules with the water molecules of ice and interactions between the probe molecules themselves. We also have to assume that there may be characteristic interaction (binding) sites on the chromophore and that temperature and constraining medium affects the probe conformational motion to such an extent that several distinct conformers are trapped.

To estimate the contribution of the inter-probe interaction, the solvatochromic parameters were measured in dichloromethane slurry, where the probe (**1**, **4**, **5**) concentrations were large enough to assume that the dipolar molecules are highly aggregated (Table 3). The concentration effect was apparent on all parameters measured. The values of E_T^N and π^* changed insignificantly, α increased by a factor of 3, and β increased by an order of magnitude, generally indicating that aggregated probes in a CH_2Cl_2 slurry (still in the presence of the solvent) exist in relatively more polar environment than those in diluted solutions. Finally, the solvatochromic parameters shown in Table 2 were used to evaluate possible probe–water and inter-probe interactions at the grain boundaries in ice under different experimental condition.

5.1. H-bond donation abilities of the probe environment (α)

The α parameter value, corresponding to the most abundant absorption band of **2** (Table 2), increased from 1.13 in liquid water to ~1.4 in ice, suggesting that H-bond donation is a more significant contributor to such polar properties of the frozen matrix than of a liquid solution. The probes **2** and **4** have no acidic hydrogens to interact with a basic moiety; however, **2** has

a negatively charged atom to make a strong H-bond with acids. Therefore, only water–probe interactions could cause high α values found in ice. In contrast, the empirical solvent polarity parameters, $E_T(33)$ (i.e., $E_T(30)$ and E_T^N), were found to be generally lower in ice (a less efficient H-bond donation) than those of liquid water. An analysis based on Eq. (2), however, indicates that only α, evaluating the environment molecules as hydrogen donors, contributed, while dipole–dipole interactions (π^*) were found negligible or not available using this technique (vide infra). Lower acceptor number values in ice, calculated from the α and $E_T(30)$ parameters, only authenticated this observation (Table 2). We are not certain about the origin of an absorption band splitting in the case of **2** (Fig. 1). Broader peaks could, moreover, represent overlaid absorption bands of more than two species. For comparison, the presence of three types of water interactions [66] and two energetically distinct binding sites for HCl [67,68] on the ice surface were reported in the temperature range of 50–140 K. It was concluded by the authors that these local surface patterns most probably interacted with the probe molecules and influenced the absorption spectra. Hydrogen bonding between water molecules of ice with self-assembled monolayers of organic compounds, such as alkanethiolate, is also known to cause a structural rearrangement of the polar terminal groups [69]. It is thus understandable that self-assembling of solvatochromic probes had to affect the hydrophobic interactions in the grain boundaries of ice.

5.2. H-bond acceptor abilities of the probe environment (β)

The parameter value, indicating the presence of electron-pair donating molecules, was found to be exceptionally high in the ice matrix (Table 2); it increased by an order of magnitude upon freezing the liquid solutions. A similar effect was, however, observed in dichloromethane slurry (Table 3). The probe **5**, in contrast to **4** (both were used to determine β), should undoubtedly be very sensitive to the presence of a base. If we assume that the increase in concentration enhances a molecular self-organization, a stronger intermolecular H-bonding among the probe molecules is the only reasonable explanation of this observation. As a result, a more efficient aggregation is expected to occur in frozen ice samples [17,27]. We, of course, cannot exclude the water–probe interactions; they were found to be dominant in the measurements of α and certainly contributed concurrently to the value of β.

5.3. Dipole–dipole interactions (π^*)

Eisenthal and co-workers applied the second harmonic spectroscopy to probe the polarity of air/water interface using *N*,*N*-diethyl-4-nitroaniline and $E_T(30)$, which was found to be nonpolar with $\pi^* = 0.22$ and $E_T^N = 0.01$ [70]. The authors concluded that the polarity of the interface between two fluids is an arithmetic average of the polarities of the constituent bulk phases. The values of π^* close to 0 obtained in this work (Table 2) may suggest that the probe molecules partially interacted with air at the grain boundaries. Contaminated polycrystalline ice is known to be substantially inhomogeneous and dynamic system [71–73], that contains air bubbles [74] and non-solid aqueous layers on the ice crystals [26,75]. The spectra of the probe **3** were resolved with large difficulties because the absorption band nearly vanished and, therefore, the interpretation of π^* should be taken with caution. Interestingly, π^* decreased in dichloromethane slurries only insignificantly, suggesting that molecular aggregation cannot be responsible for such an unexpected behavior in the frozen solutions. For comparison, π^* was found to be the most important contributor to the polar properties of the silica surfaces, followed by hydrogen-bond donation (α) by Lindley et al. [39] and the results were re-evaluated later by Spange et al. ($\pi^* = 0.38$–1.04) [40].

Our attempt to use the probes **6** and **8** has not succeeded in physically explicit explanation of a dispersed π^* values. Three different resolved λ_{max} (Fig. 5) may correspond to dipole–dipole interactions at completely different sites of the probe **8** or to different probe isomers. In such a case, a significant portion of the probe molecules provided π^* close to 0 again. Since, however, the absorption bands are of an uncertain physical origin, mainly because the probe is highly aggregated or crystallized by the freezing process in the grain boundary, the quantification of dipole–dipole interactions should be re-evaluated by other independent procedures.

5.4. Temperature effects on solvatochromic parameters

Temperature of the frozen samples did not have any major effects on the change of solvatochromic parameters (Table 2). Negligible shifts of the absorption band maxima can be caused by a decreased S/N ratio. Only abundance ratios of deconvoluted absorption bands showed minor variations which indicate that intermolecular interactions were vaguely sensitive to temperature. We recently found that methylene blue concentration increased by three orders of magnitude upon fast freezing (77 K) but by at least six orders of magnitude upon slow freezing (243 K) of its aqueous solutions [27]. Based on the results of previous research, it is presumed that a layer containing organic probes at the grain boundaries of ice was rather liquid at 253 K but fully solidified at 77 K. The probe molecules were strongly aggregated without any doubts in the whole interval of 77–253 K but the fact that the temperature and freezing conditions did not affect the solvatochromic parameters means that macroscopic molecular arrangement at the grain boundaries in the frozen solutions was not quantitatively very different, despite the fact that some parameter values are known to be temperature sensitive [76].

In conclusion, both hydrogen-bond and electron-pair donating interactions were found to be the significant contributors to the polarity of the solvatochromic probe environment in ice and, at the same time, they were larger that those measured in liquid aqueous solutions (Table 4). While the former interaction type is attributed rather to the presence of water among the probe molecules in concentrated frozen layers at the grain boundaries, the latter is probably connected with the probe aggregation (self-organization) during the freezing process. This probe behavior, however, caused considerable experimental difficulties in specifying the exclusive probe–water interactions at a fundamental

Table 4
Interactions in the grain boundaries in frozen aqueous solutions of the solvatochromic probes

Solvatochromic parameter	Interaction of a probe with	Comparing to a liquid aqueous solution, the parameter value in ice	Interpretation
α, AN	H-bond donors	Increased moderately	Water as an H-bond donor must be present
β	H-bond acceptors	Increased significantly	Enhanced molecular self-organization; inter-probe and possibly water–probe interactions
π^*	Dipolar/polarizable molecules	Decreased significantly; the results are, however, inconclusive	Specific probe interactions

level. Behavior of frozen aqueous solutions studied by the solvatochromic analysis evidently differs from that of other solid matrixes, such as rigid and acidic silica or alumina [40], and the effects observed in ice also do not parallel those found in the frozen organic solvents [32]. From the interpretation of the data obtained in this work, we can envisage the grain boundaries of ice containing organic polar impurities as a mixture of more or less organized organic/water molecular cluster, having a high degree of complexity and exhibiting specific intermolecular interactions, whose translational and conformational motion is, nevertheless, largely restricted.

The evaluation of intermolecular polar interactions in ice should be a key parameter in understanding the physics and chemistry occurring in natural ice and snow in polar regions. Continued progress in the studies of microscopic behavior of ice contaminants in ice then highlights the importance of further qualitative and quantitative laboratory experiments as complementary tools in cryospheric and polar atmospheric research.

Acknowledgments

The project was supported by the Czech Ministry of Education, Youth and Sport (MSM 0021622412) and by the Grant Agency of the Czech Republic (205/05/0819). The authors express their thanks to Jaromir Jirkovsky for his help with spectroscopy measurements. This paper contributes to the Air–Ice Chemical Interactions (AICI) task of IGAC and SOLAS. We thank Stefan Spange for providing us with the probe **7**.

References

[1] V.F. Petrenko, R.W. Whitworth, Physics of Ice, Oxford University Press, Oxford, 1999.
[2] S.B. Barone, M.A. Zondlo, M.A. Tolbert, J. Phys. Chem. A 103 (1999) 9717.
[3] B.S. Berland, M.A. Tolbert, S.M. George, J. Phys. Chem. A 101 (1997) 9954.
[4] C. Girardet, C. Toubin, Surf. Sci. Rep. 44 (2001) 163.
[5] J.T. Hoff, F. Wania, D. Mackay, R. Gillham, Environ. Sci. Technol. 29 (1995) 1982.
[6] S. Houdier, S. Perrier, F. Domine, A. Cabanes, L. Legagneux, A.M. Grannas, C. Guimbaud, P.B. Shepson, H. Boudries, J.W. Bottenheim, Atmos. Environ. 36 (2002) 2609.
[7] G.J. Kroes, D.C. Clary, Geophys. Res. Lett. 19 (1992) 1355.
[8] S. Perrier, S. Houdier, F. Domine, A. Cabanes, L. Legagneux, A.L. Sumner, P.B. Shepson, Atmos. Environ. 36 (2002) 2695.
[9] C. Guimbaud, A.M. Grannas, P.B. Shepson, J.D. Fuentes, H. Boudries, J.W. Bottenheim, F. Domine, S. Houdier, S. Perrier, T.B. Biesenthal, B.G. Splawn, Atmos. Environ. 36 (2002) 2743.
[10] P. Klan, I. Holoubek, Chemosphere 46 (2002) 1201.
[11] P. Klan, J. Klanova, I. Holoubek, P. Cupr, Geophys. Res. Lett. 30 (2003) 1313.
[12] J. Klanova, P. Klan, J. Nosek, I. Holoubek, Environ. Sci. Technol. 37 (2003) 1568.
[13] A.M. Grannas, P.B. Shepson, T.R. Filley, Global Biogeochem. Cycle 18 (2004).
[14] A.L. Sumner, P.B. Shepson, Nature 398 (1999) 230.
[15] Y. Dubowski, M.R. Hoffmann, Geophys. Res. Lett. 27 (2000) 3321.
[16] A.J. Colussi, M.R. Hoffmann, Geophys. Res. Lett. 30 (2003).
[17] M.I. Guzman, A.J. Colussi, M.R. Hoffmann, J. Phys. Chem. A 110 (2006) 931.
[18] D. Heger, J. Klanova, P. Klan, J. Phys. Chem. B 110 (2006) 1277.
[19] C.M. Roth, K.U. Goss, R.P. Schwarzenbach, Environ. Sci. Technol. 38 (2004) 4078.
[20] J.P. Devlin, V. Buch, J. Phys. Chem. 99 (1995) 16534.
[21] J.P. Devlin, J. Phys. Chem. 96 (1992) 6185.
[22] J.E. Schaff, J.T. Roberts, Langmuir 15 (1999) 7232.
[23] J.E. Schaff, J.T. Roberts, Langmuir 14 (1998) 1478.
[24] A. Borodin, O. Hofft, U. Kahnert, V. Kempter, S. Krischok, M.O. Abou-Helal, J. Chem. Phys. 120 (2004) 5407.
[25] J.P.D. Abbatt, Chem. Rev. 103 (2003) 4783.
[26] H. Cho, P.B. Shepson, L.A. Barrie, J.P. Cowin, R. Zaveri, J. Phys. Chem. B 106 (2002) 11226.
[27] D. Heger, J. Jirkovsky, P. Klan, J. Phys. Chem. A 109 (2005) 6702.
[28] W.G. Finnegan, R.L. Pitter, J. Colloid Interface Sci. 189 (1997) 322.
[29] S.R. Cohen, I. Weissbuch, R. PopovitzBiro, J. Majewski, H.P. Mauder, R. Lavi, L. Leiserowitz, M. Lahav, Isr. J. Chem. 36 (1996) 97.
[30] N. Takenaka, A. Ueda, T. Daimon, H. Bandow, T. Dohmaru, Y. Maeda, J. Phys. Chem. 100 (1996) 13874.
[31] J.G. Dash, H.Y. Fu, J.S. Wettlaufer, Rep. Prog. Phys. 58 (1995) 115.
[32] G.U. Bublitz, S.G. Boxer, J. Am. Chem. Soc. 120 (1998) 3988.
[33] A. Chowdhury, S.A. Locknar, L.L. Premvardhan, L.A. Peteanu, J. Phys. Chem. A 103 (1999) 9614.
[34] S.A. Locknar, A. Chowdhury, L.A. Peteanu, J. Phys. Chem. B 104 (2000) 5816.
[35] R. Mulvaney, E.W. Wolff, K. Oates, Nature 331 (1988) 247.
[36] M.J. Kamlet, R.W. Taft, J. Am. Chem. Soc. 98 (1976) 377.
[37] M.S. Antonious, E.B. Tada, O.A. El Seoud, J. Phys. Org. Chem. 15 (2002) 403.
[38] C. Reichardt, Chem. Rev. 94 (1994) 2319.
[39] S.M. Lindley, G.C. Flowers, J.E. Leffler, J. Org. Chem. 50 (1985) 607.
[40] S. Spange, E. Vilsmeier, Y. Zimmermann, J. Phys. Chem. B 104 (2000) 6417.
[41] X.Y. Zhang, M.M. Cunningham, R.A. Walker, J. Phys. Chem. B 107 (2003) 3183.
[42] J.J. Michels, J.G. Dorsey, Langmuir 6 (1990) 414.
[43] S. Spange, C. Schmidt, H.R. Kricheldorf, Langmuir 17 (2001) 856.
[44] E.B. Tada, L.P. Novaki, O.A. El Seoud, J. Phys. Org. Chem. 13 (2000) 679.
[45] C. Laurence, P. Nicolet, M.T. Dalati, J.L.M. Abboud, R. Notario, J. Phys. Chem. 98 (1994) 5807.
[46] M. El-Sayed, H. Muller, G. Rheinwald, H. Lang, S. Spange, J. Phys. Org. Chem. 14 (2001) 247.
[47] S. Spange, D. Keutel, Liebigs Annalen der Chemie (1992) 423.
[48] A.R. Katritzky, D.C. Fara, H.F. Yang, K. Tamm, T. Tamm, M. Karelson, Chem. Rev. 104 (2004) 175.
[49] Y. Marcus, Chem. Soc. Rev. 22 (1993) 409.

[50] Y. Marcus, J. Solution Chem. 20 (1991) 929.
[51] C. Reichardt, Pure Appl. Chem. 76 (2004) 1903.
[52] C. Reichardt, D.Q. Che, G. Heckenkemper, G. Schafer, Eur. J. Org. Chem. (2001) 2343.
[53] C. Reichardt, M. Eschner, G. Schafer, J. Phys. Org. Chem. 14 (2001) 737.
[54] P. Nicolet, C. Laurence, J. Chem. Soc.-Perkin Trans. 2 (1986) 1071.
[55] G. Gritzner, J. Mol. Liq. 73/74 (1997) 487.
[56] C. Laurence, P. Nicolet, M. Helbert, J. Chem. Soc.-Perkin Trans. 2 (1986) 1081.
[57] U. Mayer, Pure Appl. Chem. 41 (1975) 291.
[58] U. Mayer, Pure Appl. Chem. 51 (1979) 1697.
[59] Kindly provided by Prof. S. Spange.
[60] V. Petrov, L. Antonov, H. Ehara, N. Harada, Comp. Chem. 24 (2000) 561.
[61] L. Antonov, Trac-Trend. Anal. Chem. 16 (1997) 536.
[62] R.A. Morton, J. Chem. Soc. 907 (1934) 901.
[63] R.W. Soukup, R. Schmid, J. Chem. Educ. 62 (1985) 459.
[64] M.J. Kamlet, J.L.M. Abboud, M.H. Abraham, R.W. Taft, J. Org. Chem. (1983) 2877.
[65] Anonymous referee's communication.
[66] B. Rowland, N.S. Kadagathur, J.P. Devlin, V. Buch, T. Feldman, M.J. Wojcik, J. Chem. Phys. 102 (1995) 8328.
[67] V. Buch, J. Sadlej, N. Aytemiz-Uras, J.P. Devlin, J. Phys. Chem. A 106 (2002) 9374.
[68] S.C. Park, H. Kang, J. Phys. Chem. B 109 (2005) 5124.
[69] I. Engquist, M. Lestelius, B. Liedberg, J. Phys. Chem. 99 (1995) 14198.
[70] H.F. Wang, E. Borguet, K.B. Eisenthal, J. Phys. Chem. B 102 (1998) 4927.
[71] J.S. Wettlaufer, Phys. Rev. Lett. 82 (1999) 2516.
[72] J.S. Wettlaufer, Interface Sci. 9 (2001) 117.
[73] J.S. Wettlaufer, M.G. Worster, Annu. Rev. Fluid Mech. 38 (2006) 427.
[74] J.A. Killawee, I.J. Fairchild, J.L. Tison, L. Janssens, R. Lorrain, Geochim. Cosmochim. Acta 62 (1998) 3637.
[75] A. Doppenschmidt, H.J. Butt, Langmuir 16 (2000) 6709.
[76] E. Bosch, M. Roses, K. Herodes, I. Koppel, I. Leito, V. Taal, J. Phys. Org. Chem. 9 (1996) 403.